The authors have developed a high-resolution 3D wind field dataset (YRD1km) over the Yangtze River Delta by running WRF driven by ERA5 reanalysis, assimilating observations, and updating land-use information. This dataset addresses a significant lack of high-resolution, 3D wind products in this important region during the summer months. However, the manuscript still has several structural and methodological issues. Therefore, I recommend that it be considered for publication only after major revision.

We sincerely thank the reviewer for the thoughtful and constructive comments. We have carefully considered each point and revised the manuscript accordingly. Detailed responses to all comments are provided below.

Comments:

1. The manuscript evaluates the dataset mainly using MAE / RMSE / NSE, but the verification metrics used in Figures 5 and 6 appear inconsistent with those used elsewhere. Unless there is a justified reason for deviation, please ensure that the verification metrics are consistent throughout the manuscript. If this is not possible, please provide an explanation in the methods section or the figure captions.

   Response: Thank you for this thoughtful comment. In our original manuscript, we aimed to maintain consistency in the statistical metrics and initially calculated and plotted MAE, RMSE, and NSE. Upon analyzing their temporal variations, we observed that MAE and RMSE exhibited highly similar trends. To present the results more clearly, we therefore retained only MAE and NSE in the figures. A similar relationship was observed for the vertical validation in Figure 5. We fully understand that this simplification may have caused confusion, and we sincerely appreciate your suggestion for greater consistency. In response, we have revised Figures 5 and 6 accordingly. Specifically, RMSE has been added to Figure 5, and Bias in Figure 6 has been replaced by MAE to align with the evaluation framework used elsewhere in the manuscript.

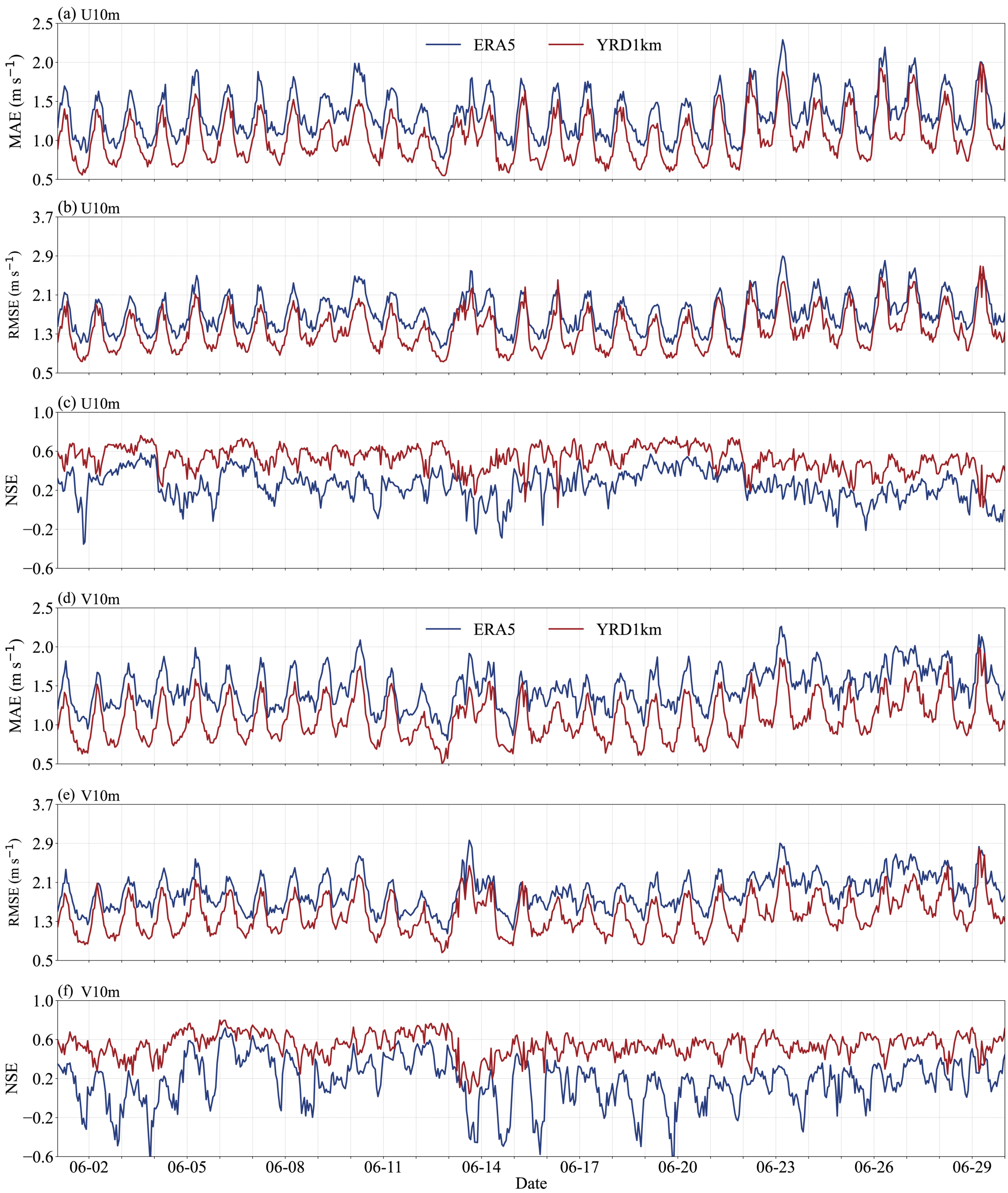

Figure 5. Time series of model performance metrics for hourly 10-m wind components over the YRD region in June 2022. Panels (a), (b) and (c) show the MAE, RMSE and NSE, respectively, for the U10m. Panels (d), (e) and (f) show the corresponding MAE, RMSE and NSE metrics for the V10m. The red and blue lines represent the YRD1km and ERA5 datasets, respectively.

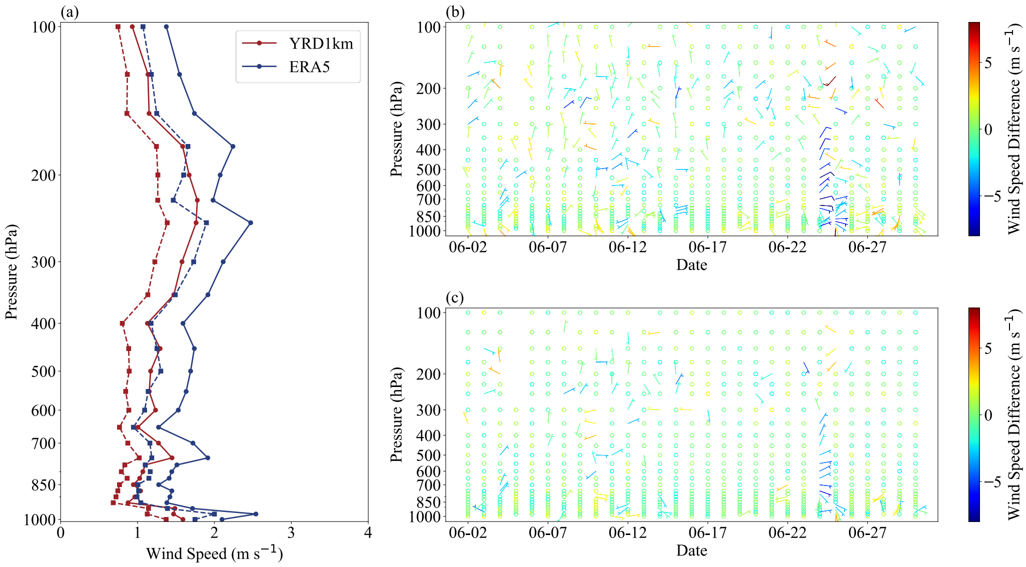

Figure 6. Vertical evaluation of wind field performance from the YRD1km and ERA5 datasets against radiosonde observations at the Baoshan station in Shanghai during June 2022. (a) Vertical profiles of wind speed MAE (dashed lines) and RMSE (solid lines) for YRD1km (red) and ERA5 (blue), calculated from all available soundings at 00 and 12 UTC. (b) Time–height cross-section of wind vector differences between ERA5 and radiosonde observations (RAOB), with wind speed differences (m/s) indicated by color shading. (c) As in (b), but for YRD1km minus RAOB. Wind difference plots are shown at 24-hour intervals, beginning at 00 UTC on 2 June 2022.

2. The text in lines 242–257 appears to be duplicated. Please check the manuscript carefully and remove any redundant content.

   Response: We sincerely appreciate your careful reading and for pointing out this duplication. We have removed the redundant paragraph, which provides a clearer and more concise description of the validation process.

3. The manuscript's validation focuses on 10-m near-surface winds, a single radiosonde station, and an individual case study, which is insufficient to demonstrate the three-dimensional characteristics of the dataset.

   Response: Thank you for this valuable comment. We fully agree that a convincing demonstration of the three-dimensional characteristics of the YRD1km dataset is essential. In the revised manuscript, we have clarified and substantially strengthened the evidence supporting its 3D performance through complementary vertical statistics, multi-station evaluations, and physically consistent case-based analyses.

As shown in the updated Figure 6a, the manuscript now presents vertical evaluations of wind fields at multiple pressure levels, revealing systematic reductions in MAE and RMSE throughout the tropospheric column (1000–100 hPa). These improvements indicate that YRD1km effectively captures both near-surface and upper-level wind structures. Together with the time–height cross-sections in Figures 6b and 6c, these results demonstrate that YRD1km reproduces the vertical stratification and temporal evolution of winds more realistically than ERA5. To further assess the representativeness of the vertical performance, we conducted similar validations from all valid sounding samples at 11 radiosonde stations across the Yangtze River Delta are now presented in Figure S1. These statistics show robust and systematic improvements of YRD1km relative to ERA5, including average reductions of approximately 30% in MAE, 28% in RMSE, and increases of about 48% in NSE, demonstrating enhanced vertical wind representation across the entire troposphere.

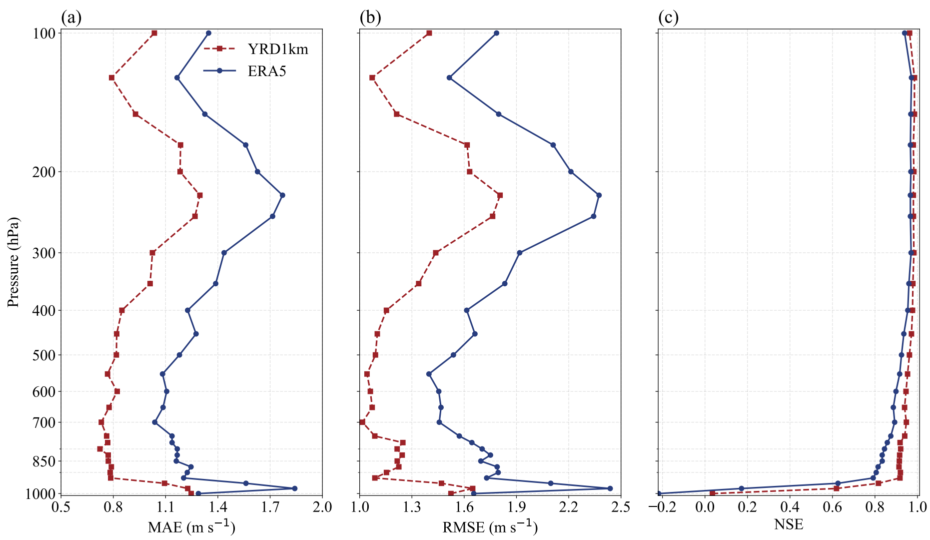

Figure S1. Vertical evaluation of wind field performance from the YRD1km and ERA5 datasets against radiosonde observations at all 11 stations across the Yangtze River Delta in June 2022. Panels show (a) MAE, (b) RMSE and (c) NSE, computed using all available 00 UTC and 12 UTC soundings.

Regarding the concern that the manuscript relies on an individual case study, we emphasize that the convective event analyzed is not intended as standalone evidence, but rather as a physically interpretable illustration of the dataset's three-dimensional dynamical consistency. To further address this concern, we additionally include an independent mesoscale convective precipitation event that occurred over the study region from 04 to 12 UTC on 10 June 2022. During the early stage (04–06 UTC), precipitation was characterized by localized and discrete convective cells, which intensified and organized into a southwest–northeast-oriented rainband during 07–08 UTC, followed by gradual weakening thereafter (08–12 UTC; Figure S2).

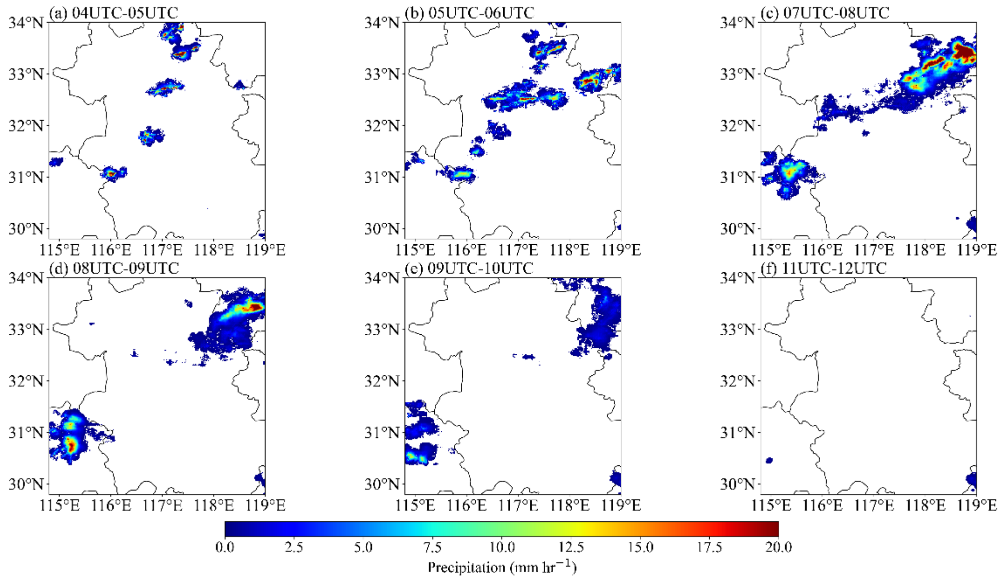

Figure S2. Hourly precipitation evolution during the convective event on 10 June 2022 (04–12 UTC).

Multi-level dynamical analyses reveal that YRD1km captures the evolving 3D wind structures associated with this event more realistically than ERA5. At 500 hPa, ERA5 depicts a relatively uniform westerly–northwesterly flow, whereas YRD1km resolves finer-scale mesoscale features, including enhanced wind speed gradients and weak shear, whose spatial configuration aligns well with the subsequent orientation of the precipitation band. At 700 hPa, ERA5 exhibits generally weak winds and indistinct dynamical lifting signals, while YRD1km identifies localized wind speed enhancements and weak convergence zones that spatially coincide with regions of intense rainfall. At 850 hPa, although ERA5 represents the background southeasterly inflow, the low-level jet structure and convergence patterns are poorly defined. In contrast, YRD1km clearly resolves a low-level jet and a pronounced deceleration zone along its leading edge, forming a low-level convergence region that closely corresponds to the location of the strongest precipitation during 07–08 UTC (Figure S3). These features highlight the role of low-level jet dynamics and associated convergence lifting in the initiation and intensification of the convective system.

Taken together, the expanded multi-station vertical statistics, regionally aggregated sounding evaluations, and the physically consistent multi-level analysis of a representative convective event collectively demonstrate that YRD1km provides dynamically coherent and regionally representative three-dimensional wind fields across spatial, temporal, and vertical dimensions.

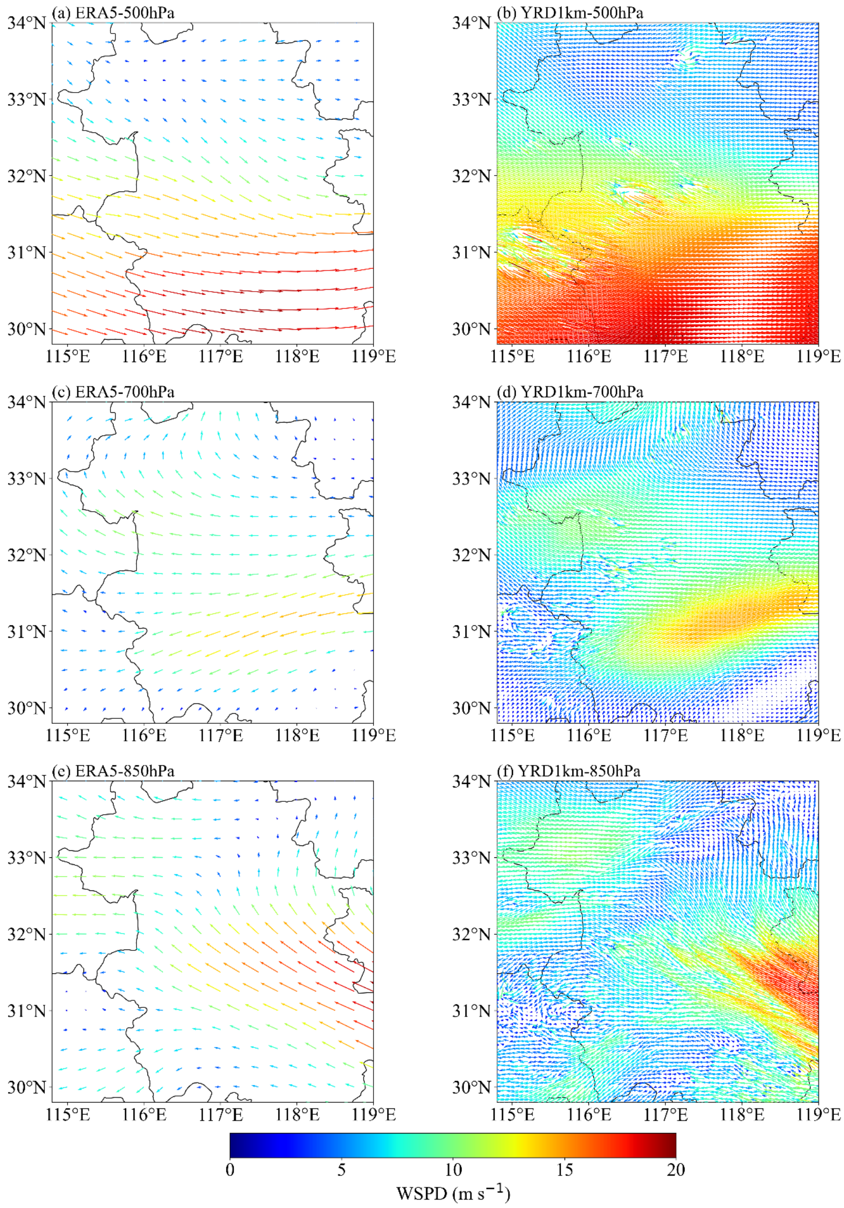

Figure S3. Comparative analysis of horizontal wind field structures between the ERA5 and YRD1km datasets during the mesoscale convective precipitation event over the study region. Shown are horizontal wind vectors (arrows) and wind speed (color shading) at the (a, b) 500 hPa, (c, d) 700 hPa, and (e, f) 850 hPa levels from ERA5 (left column) and YRD1km (right column) at 04:00 UTC on 10 June 2022, corresponding to the mature stage of the convective system. For visual clarity, wind vectors in YRD1km are thinned by a factor of six.

4. Please ensure that abbreviations are standardised throughout the manuscript (e.g., "EWC2020" and "ESA2020").

   Response: Thank you for your suggestion. We have carefully reviewed the entire manuscript and standardised all abbreviations related to the land use dataset. Specifically, we now uniformly use EWC2020 to denote the ESA WorldCover 2020 land use data and this form is consistently applied throughout the manuscript, including figures, tables, and text.

5. The manuscript states that YRD1km uses 61 vertical model levels, whereas line 400 refers to 32 standard levels. Are the 32 standard levels a subset of the 61 model levels, or are they obtained by interpolation? A clear description of the vertical level and the interpolation method should be provided.

   Response: Thank you for this helpful comment. The 32 standard pressure levels are obtained through vertical interpolation from the original 61 terrain-following eta levels of the WRF model, rather than being a direct subset. We have added a clear description of this process in Section 4.3 to clarify the relationship between the model levels and the interpolated standard levels.

6. Table 1 and Figure 3 only present results for a single day, which may be affected by temporary weather conditions. To obtain more robust conclusions, longer time periods should be included.

   Response: Thank you for this valuable comment. Table 1 and Figure 3 were designed as representative examples to illustrate the dataset's capability in resolving mesoscale wind structures and near-surface dynamics on a typical summer day. We acknowledge that wind field performance may vary under different weather conditions and at different times. To address this concern and ensure the robustness of our conclusions, we have complemented the single-day analysis with long-term statistical evaluations. Specifically, Section 4.2 presents month-long hourly time series of MAE, RMSE, and NSE for June 2022 (Figures 5), covering all days and synoptic conditions during the period. These results demonstrate consistent error characteristics and performance advantages of YRD1km over ERA5 across the entire month.

Together, the long-term evaluations confirm that the results shown in Table 1 and Figure 3 are representative rather than case-specific, and that the conclusions drawn for the dataset remain robust across varying temporal and meteorological conditions.

Thank you for this valuable comment. Table 1 and Figure 3 were designed as representative examples, based on a total of 8,107 samples, to illustrate the dataset's capability in resolving mesoscale wind structures and near-surface dynamics on a typical summer day. We acknowledge that wind field performance may vary under different weather conditions and at different times. To address this concern and ensure the robustness of our conclusions, we have complemented the single-day analysis with long-term statistical evaluations. Specifically, Section 4.2 presents month-long hourly time series of MAE, RMSE, and NSE for June 2022 (Figure 5), encompassing all days and a wide range of synoptic conditions during the period. These results demonstrate consistent error characteristics and sustained performance advantages of YRD1km over ERA5 throughout the month.

Taken together, the long-term evaluations confirm that the results shown in Table 1 and Figure 3 are representative rather than case-specific, and that the conclusions drawn for the dataset remain robust across varying temporal and meteorological conditions.

7. Please specify the number of training and testing samples in Table 3 or in the methods section, and describe the sampling strategy. The results of independent validation with withheld stations should also be presented.

Response: Thank you for these valuable suggestions. In response, we have revised the manuscript to explicitly describe the independent validation strategy and the associated sampling procedure.

Specifically, approximately 10% of the AWS stations were randomly withheld from the observational nudging process and reserved exclusively for independent validation. Among the total 362 AWS stations, 36 stations were withheld for validation, while the remaining 326 stations were retained to provide observational constraints for the WRF simulations. To ensure that the evaluation captures a representative range of synoptic and mesoscale meteorological conditions, the independent validation was conducted over a continuous four-day period (1–4 June 2022). Results from the withheld stations show that the YRD1km dataset consistently outperforms ERA5 in simulating the 10-m wind field (Figure S4). For the U component, NSE increases by 5.08%, while MAE and RMSE decrease by 4.80% and 3.01%, respectively, relative to ERA5. For the V component, NSE increases by 10.11%, with corresponding reductions of 8.09% in MAE and 5.14% in RMSE. In addition, the fitted relationships between simulated and observed U and V components show a noticeably closer alignment with the 1:1 reference line (Figure S4), indicating improved fidelity in reproducing near-surface wind variability. These results demonstrate that YRD1km maintains superior predictive performance even at stations that were not included in the assimilation process.

Overall, these revisions explicitly clarify the sampling strategy and present robust independent validation results, thereby reinforcing the reliability of the proposed methodological framework and the robustness of the resulting dataset.

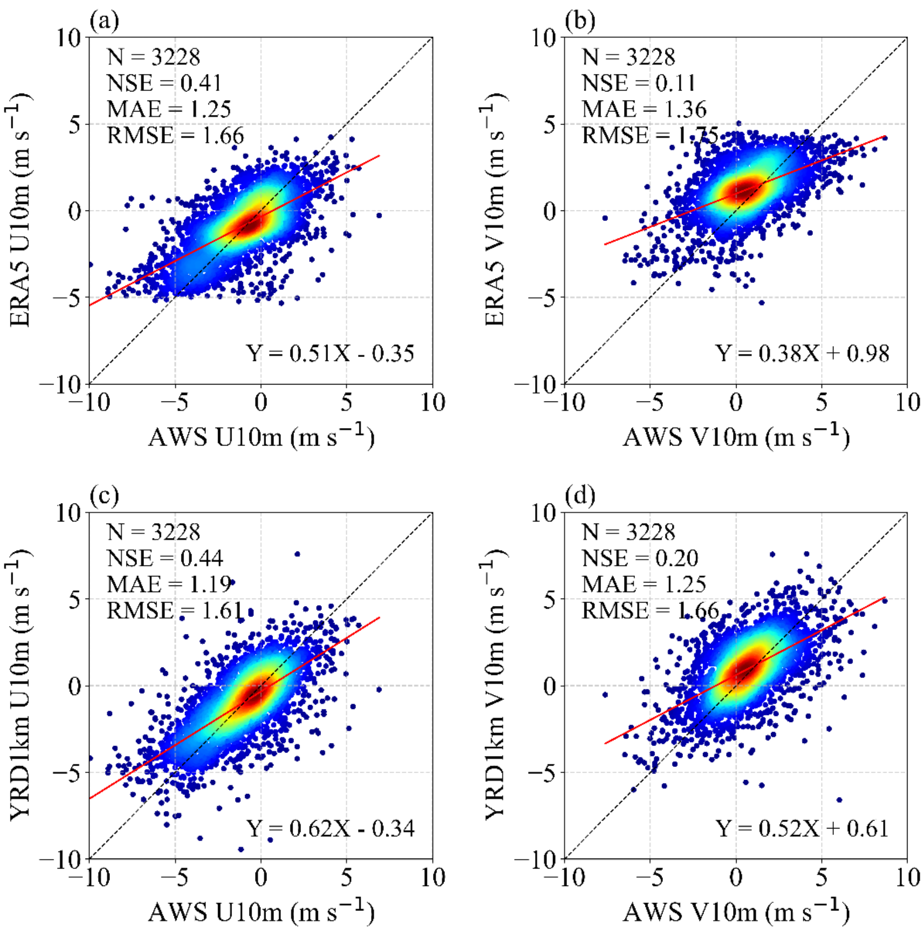

Figure S4. Independent validation scatterplots of 10-m wind components over the YRD region: (a) ERA5 U10m, (b) ERA5 V10m, (c) YRD1km U10m, and (d) YRD1km V10m.

8. For the Baoshan station used in validation, please provide the station metadata (latitude and longitude, elevation, and underlying surface/land-use).

Response: Thank you for your valuable comment. We have added the Baoshan radiosonde station metadata to Section 4.3. The Baoshan station (ID:58362) is located at 31.39° N, 121.45° E, with an elevation of 3.3 m. The site is situated in a densely built-up urban area (Urban and Built-Up), consistent with the EWC2020 land-cover classification shown in Figure 1.

9. When validating in mountainous and lake regions (e.g., Figure 4), please include terrain/lake contours or DEM information in the maps to make them clearer.

Response: Thank you for this constructive suggestion. Figure 4 already included terrain elevation shading to illustrate the mountainous topography, where darker tones indicate higher altitudes. To further improve the visual distinction of lake areas, we have added steelblue shaded overlays for major lakes (e.g., Lake Taihu). The updated figure now more clearly distinguishes mountainous and lake regions, facilitating interpretation of local wind variations.

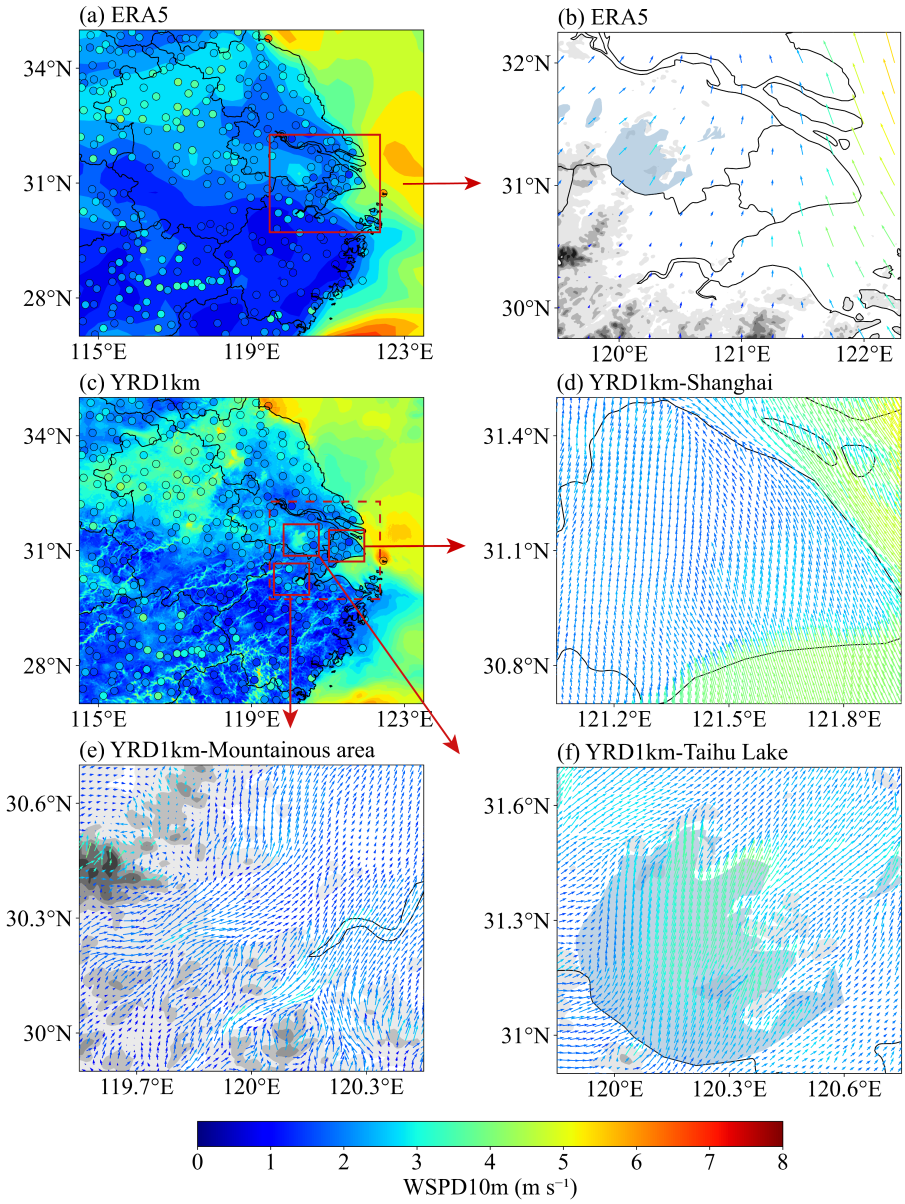

Figure 4. Spatial distribution of daily mean near-surface wind fields over the YRD region on 1 June 2022. Panels (a) and (c) show daily mean 10-m wind speed (WSPD10m) from the ERA5 and YRD1km datasets, respectively, overlaid with AWS station observations (colored dots). Panels (b), (d), (e), and (f) show locally enlarged wind vector fields: (b) ERA5 over Shanghai and its surrounding urban agglomeration; (d) YRD1km over the Shanghai metropolitan area;

(e) the mountainous region near Hangzhou; and (f) Lake Taihu. Arrows are color-coded by wind speed magnitude and overlaid on shaded terrain elevation, with darker tones indicating higher altitudes. Major water bodies are shaded in steelblue for clearer identification.

10. Please ensure that the numerical precision and formatting are consistent throughout the manuscript (e.g., 26% in Lines 199 and 46.67% in Table 3).

    Response: Thank you for pointing out this inconsistency. We have carefully checked all numerical values throughout the manuscript and standardised the precision and formatting. Percentages are now expressed consistently with two decimal places (e.g., 26.67%) unless used as approximate descriptive values (e.g., "about 26%").

11. The data download link provided in the abstract points to files that are currently unavailable for download.

    Response: Thank you for raising this concern. The dataset is currently hosted on ScienceDB with a DOI link already assigned. To comply with the repository's policy and ESSD data access requirements, the dataset has been made accessible to the editor and reviewers through a private review link during the peer-review process. The dataset will be formally released and publicly accessible immediately upon the paper's publication, at the same DOI link provided in the manuscript.